Designing Piezoelectric Interdigitated Microactuators using COMSOL

Oliver J. Myers[*1], M. Anjanappa[2] and C. Freidhoff [3]
[1] Mississippi State University, [2]University of Maryland Baltimore County, [3]Northrop Grumman Corporation, Electronics Systems Sector, Baltimore, MD
*Corresponding author: 219 Carpenter Hall, Box 9552, Mississippi State, MS 39762, myers@me.msstate.edu

Abstract: This paper presents a methodology towards designing, analyzing and optimizing piezoelectric interdigitated microactuators using COMSOL Multiphysics. The models used in this study were based on a circularly interdigitated design that takes advantage of primarily the d_{33} electromechanical piezoelectric constant coefficient. Because of the symmetric nature of the devices, a small number of 2-D axi-symmetric models were developed to characterize the behavior of the diaphragms. The variation in the design parameters and their effect on deflection was captured using these models. The models also showed that several of the design parameters were naturally coupled. Discrete models were then used to capture the variations in key design parameters during fabrication. The numerical models correlate well to the maximum deflection of the experimental devices.

Keywords: Microactuators, piezoelectric, modeling.

1. Introduction

Micromechanical devices that employ active piezoelectric materials, typically in thin-film form, show promise for a variety of applications, particularly actuation [1,2]. As the devices become increasingly diverse and sophisticated, the need arises for increasingly accurate and efficient modeling of their behavior for design purposes. The electrically active region of the piezoelectric material performs either as a sensor (strain input, electrical output) or as an actuator (electric-field input, displacement output) or both. The piezoelectric layer is usually a deposited film with active-area dimensions that are 100X or more than the thickness. Other electrically active and passive layers are present and overlap each other to form geometrically and functionally complex layered structures. Since the devices are on the micro-scale, the active part of the structure makes its behavior more sensitive to electrical aspects of its environment; hence good electrical modeling is required [3]. The task of designing and optimizing microactuators or MEMS devices brings unique challenges of analyzing interdependent physical phenomena, device sensitivity and small scale geometries. MEMS simulation requires multi-disciplinary software to capture the multi-physical nature of MEMS devices [4].

This paper presents the design initiation of interdigitated piezoelectric thin-film mico-actuators. Parametric analysis is initially used to gather a large battery of solutions from a few models. Experiments were then conducted on discrete actuators with varying center disk diameters and electrode patterns. Finite element models of the particular actuator diaphragms were created to corroborate the experimental observations.

2. Theoretical Background

2.1 Elasticity Equations

The deflection model of the interdigitated membrane begins with the equation for elastic deflection:

$$w = \frac{q}{64D}\left(a^2 - r^2\right) \qquad (1)$$

where q is the pressure, D is the flexural rigidity, a is the radius and r is the radial position. Taking this equation a step further, the shear component is introduced to account for interfacial effect of the layers.

$$w = \frac{q}{64D}\left(\left(a^2 - r^2\right) + \frac{4h^2}{1-\nu}\left(a^2 - r^2\right)\right) \qquad (2)$$

where h is the thickness and ν is the Poisson's ratio of the plate. Accounting for the multiple layers, equivalent D, ν, were derived as:

$$D_{e=} = \frac{E_e h^3}{12(1-\nu_e)} K_{2e} \quad (3)$$

$$\nu_e = \nu_a \frac{K_{3e}}{K_{2e}} \quad (4)$$

$$E_e I = \frac{w t_b^3 t_a E_b E_a}{12(t_a E_a + t_b E_b)} K_{1e} \quad (5)$$

2.2Piezoelectric Constitutive Equations

Piezoelectricity is the interaction between electrical fields and mechanics. To obtain a reasonable model of this interaction, linear elasticity equations are coupled with electrostatic charge equations by means of electric constants. The stress-charge form of the equations is:

$$\begin{bmatrix} S \\ D \end{bmatrix} = \begin{bmatrix} s^E & d_t \\ d & \varepsilon^T \end{bmatrix} \begin{bmatrix} T \\ E \end{bmatrix} \quad (6)$$

where S is the strain, s^E is the compliance matrix at a constant electric field, d_t is transpose of the piezoelectric coupling matrix relating strain to electric field, ε^T is the permittivity at constant stress, T is the stress, E is the electric field and D is the electric displacement. The stress-charge form of these equations is more useful for finite element analysis because the stress-charge form matches the PDEs for Navier's equations for mechanical stress and Gauss' law of electric charge. The equations of conversion are as follows:

$$c^E = \left[s^E\right]^{-1} \quad (7)$$

$$e = d\left[s^E\right]^{-1} \quad (8)$$

$$\varepsilon^S = \varepsilon^T - d\left[s^E\right]^{-1} d_t \quad (9)$$

where c^E is the stiffness matrix, e is the piezoelectric coupling matrix relating stress to electric field and e^S is the permittivity matrix at constant strain. The stress-charge form is then:

$$\begin{bmatrix} T \\ D \end{bmatrix} = \begin{bmatrix} c^E & -e_t \\ e & \varepsilon^S \end{bmatrix} \begin{bmatrix} S \\ E \end{bmatrix} \quad (10)$$

3. Initial Model Design Parameters

Initial models were created with the materials listed in Table 1. The measured residual stresses induced from fabrication were also incorporated into the models as shown in figure 1 [5].

Table. Material Properties [6,7,8,9]

Material	E (GPa)	ν	ρ (kg/m3)
Gold	80	0.42	19280
ZrO2	86	0.27	4600
SiO2	74.5	0.17	2200
Al2O3	376.91	0.24	3895

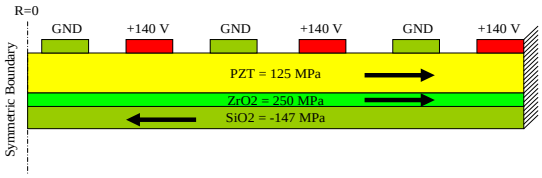

Figure 1. Residual stress boundary conditions

The model variations include material thickness with an emphasis on piezoelectric thickness, electrode width, electrode separation and center disk diameter.

Simulations were conducted to determine a viable piezoelectric material thickness for these diaphragms. Figure 2 shows the sharp decline in deflection with respect to material thickness as the piezoelectric material is increased from 2 to 3μm.

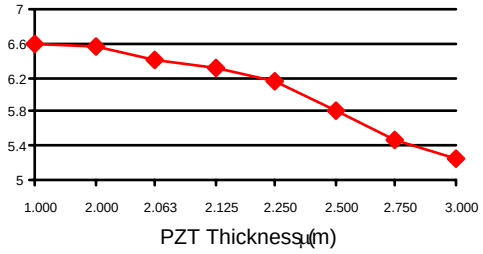

Figure 2. Deflection vs. piezoelectric material thickness

Models were also created to simulate the various clamping conditions that were anticipated during the fabrication and release processes of these diaphragms. These boundary conditions included a clamped boundary at the outer circumference of the diaphragm, a clamped boundary with an offset electrode pattern, a partially clamped electrode and a fully clamped electrode. The results of figure 3 show that each of the specific boundary conditions gave a slight progressive decrease in deflection.

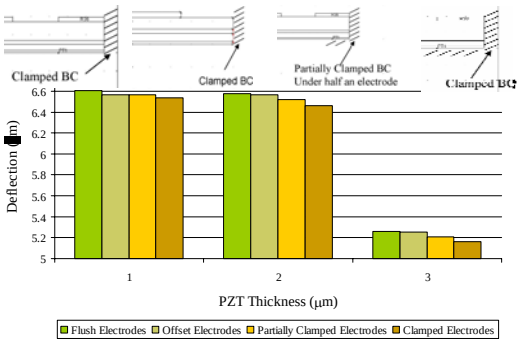

Figure 3. Deflection vs Clamping Boundary Conditions

Electrode separation models and varied center disk diameter models showed a natural coupling with the number of electrodes and further highlighted a deflection that was dependent on the number of electrodes. As the pitch increased, the deflection increased, however the deflection further increased for diaphragms with an even number of electrodes. Even though the increasing center diameter had a negative effect on the deflection, the same variance between an even and odd number of electrodes was predicted.

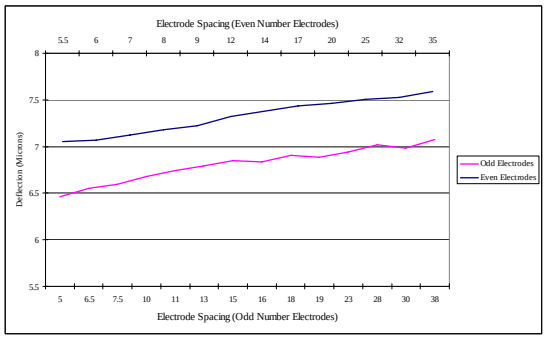

Figure 4. Deflection vs. electrode separation

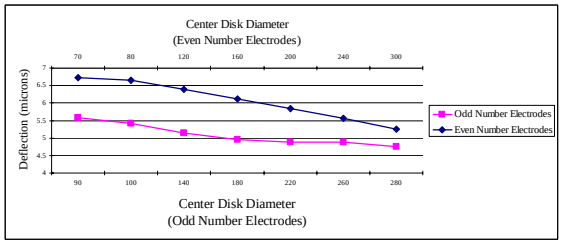

Figure 5. Deflection vs. center disk diameter

4. Experimental Validation

The ZYGO NewView 100 White Light Profilometer was used to observe the static deflection of the micro-actuators with experimental setup as shown in Figure 10. Data was collected by varying the applied DC voltage from 0 to 180V. The polarity of the applied voltage was set at positive on the interior electrodes. The samples were poled at approximately three times the Curie voltage ($3Vc$), which is 100V for 15 minutes [10]. Simulations of the above interdigitated designs were run varying the voltage between 0 and 180V and incorporated the residual stress data as applied to the previous simulation models. The polarities will also be set in the same manner as the experiments.

Figure 6. Static Deflection Measurement Setup

The experiments were conducted on a set of membranes that were made of Al_2O_3, SiO_2, ZrO_2 and PZT. These membranes were 650μm in diameter with center disk diameters of 90, 150, and 210μm. The electrodes and center disk covered 80 percent of the membrane with a 5μm width and pitch. The number of electrodes for each membrane ranged from 15 to 21 with respect to the center disk. Data was collected only at 100, 140 and 180V to get a sense of the effect of the number of electrodes and center disk. The electrodes were polarized so the positive potential was on the electrode just inside the outermost electrode which correlated with the experimental procedure used. The center disk was not activated.

5. Discussion

These membranes experienced a great amount of deflection because the 0.25μm thick protective layer of Al_2O_3 was sputtered which allowed for good manufacturing tolerancing, good adhesion to itself and to the SiO_2 layer.

5.1 650μm Membrane with 90μm Center Disk

The experimental deflection values of the 90μm Center Disk membrane were 3.93, 6.44 and 7.93μm for 100, 140, and 180 Volts respectively. When corrected simulations were conducted, the residual stresses in the piezoelectric material only appeared to be relevant at 100 V and the residual stresses of the ZrO_2 and SiO_2 were relevant at 140 and 180V. This only partially corresponds to the data Penn State gathered. The residual stresses were measured only after the membranes have been released. The silicon layer also crosses the stress threshold from being compressive to tensile at a voltage before 100V, the zirconium layer greatly increases in tension and the piezoelectric material does not appear to be as tensile as initially determined.

Table 1: Residual Stress Values Applied During Numerical Analysis of 650μm Diameter Actuator with 90 μm Center Disk.

Voltage	ZrO_2	SiO_2	PZT
100 V	270 MPa	206 MPa	60 MPa
140 V	350 MPa	245 MPa	0 MPa
180 V	400 MPa	305 MPa	0 MPa

The experimental deflection as shown in **Figure 7** shows a flattened center and an inconsistent curve along the radius of the membrane where the numerical simulations show a curved center deflection and small stair step pattern along the radius of the membrane where the electrodes are positioned.

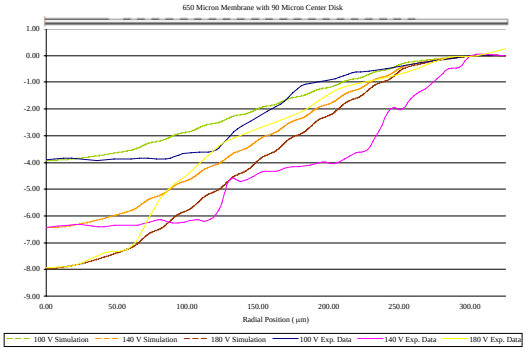

Figure 7. Corrected Numerical versus Experimental Deflection Comparison of 650 Micron Diameter Actuator with 90 Micron Center Disk

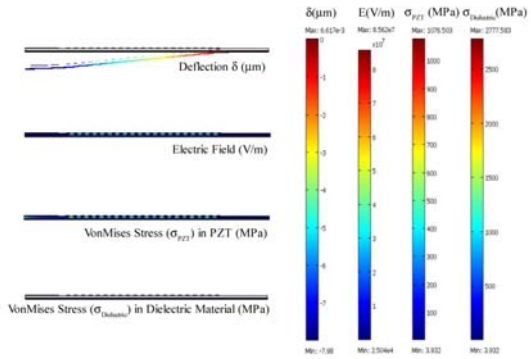

Figure 8. Correlation of Numerical Deflection, Electric Field, and Von Mises Stresses in 650 Micron Diameter Membrane with 90 Micron Center Disk at 180 Volts

5.2 650μm Membrane with 150μm Center Disk

The experimental deflection values of the 150 μm Center Disk membrane were 2.12, 5.86 and 7.17 μm for 100, 140, and 180 Volts respectively. When corrected simulations were conducted, the residual stresses of the piezoelectric material, again, only appeared to be relevant at 100 V and the residual stresses of the ZrO_2 and SiO_2 were relevant at all voltages. The silicon layer also crosses the stress threshold from being compressive to tensile at a voltage before 100V and the piezoelectric material does appear to be as tensile as initially determined.

Table 2: Residual Stress Values Applied During Numerical Analysis of 650µm Dia. with 90 µm Center Disk Actuator

Voltage	ZrO_2	SiO_2	PZT
100 V	270 MPa	205 MPa	130 MPa
140 V	360 MPa	255 MPa	0 MPa
180 V	410 MPa	315 MPa	0 MPa

The experimental deflection as shown in **Figure 9** shows a flattened center and an inconsistent curve along the radius of the membrane where the numerical simulations show a curved center deflection and small stair step pattern along the radius of the membrane where the electrodes are positioned.

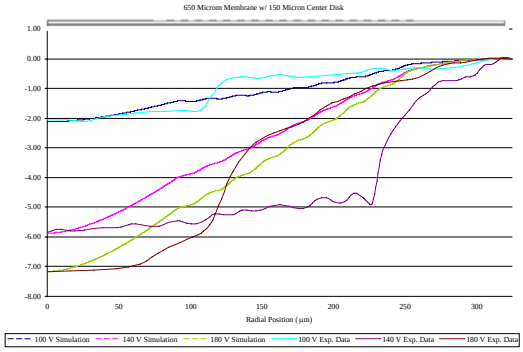

Figure 9. Corrected Numerical versus Experimental Deflection Comparison of 650 Micron Diameter Actuator with 150 Micron Center Disk

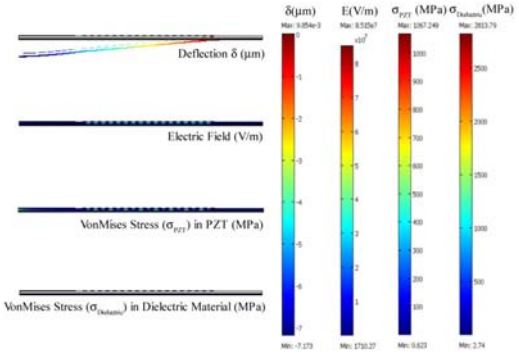

Figure 10. Correlation of Numerical Deflection, Electric Field, and VonMises Stresses in 650 Micron Diameter Membrane with 90 Micron Center Disk at 180 Volts

6.3 650µm Membrane with 210µm Center Disk

The experimental deflection values of the 210 µm Center Disk membrane were 1.44, 1.45 and 1.40 µm for 100, 140, and 180 Volts respectively as shown in Figure 11. When corrected simulations were conducted, the residual stresses of the piezoelectric material only appeared to be relevant at 140 and 180V and the residual stresses of the ZrO_2 and SiO_2 were relevant 100 and 140V. This does not correspond to the data Penn State gathered. The residual stresses of all the materials were significantly lower than initially determined. The large center disk and lack of electrodes caused the actuator to behave as a sandwich piezoelectric unimorph that utilized the d_{31} electromechanical coupling coefficient rather than the desired d_{33} coupling coefficient.

Table 3: Residual Stress Values Applied During Numerical Analysis of 650µm Dia. with 90 µm Center Disk Actuator

Voltage	ZrO_2	SiO_2	PZT
100 V	29 MPa	29 MPa	0 MPa
140 V	30 MPa	35 MPa	30 MPa
180 V	400 MPa	305 MPa	30 MPa

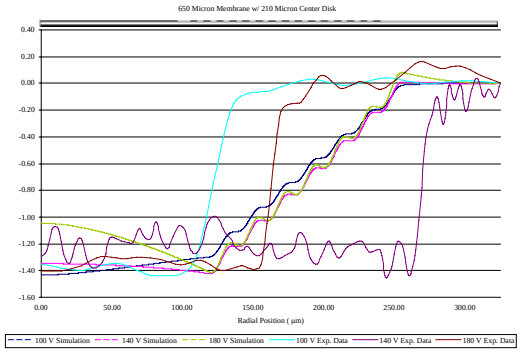

Figure 11. Corrected Numerical versus Experimental Deflection Comparison of 650 Micron Diameter Actuator with 210 Micron Center Disk

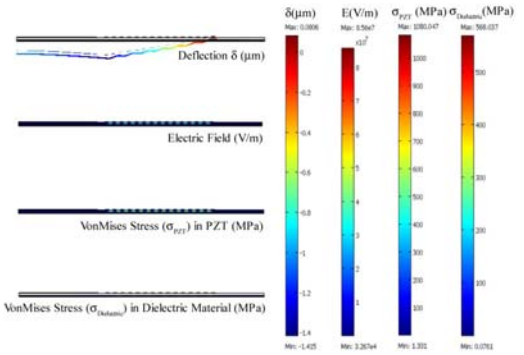

Figure 12. Correlation of Numerical Deflection, Electric Field, and Von Mises Stresses in 650 Micron Diameter Membrane with 90 Micron Center Disk at 180 Volts

7. Conclusions

A design and analysis methodology using 2-D axis-symmetric multi-physical models is developed for circularly interdigitated piezoelectric micro-actuators. Key physical design parameters were varied using the embedded designing module and the materials and corresponding properties were also varied to gain an understanding of which materials are best suited for the application. Experiments were conducted on a discrete set of microactuators that naturally coupled the center disk diameter and number of electrodes. Good deflection correlation was obtained between the numerical and limited experimental data, however more work needs to be done numerically to better replicate the shape functions of these particular devices. The numerical models can serve as an active design tool to optimize interdigitated piezoelectric microactuator membranes for various applications.

8. References

1. B. Chen, B. Cheeseman, A. Safari, S. Danforth, and T. Chou, Theoretical and numerical predictions of the electromechanical behavior of spiral-shaped lead zirconate titanate (pzt) actuators, *IEEE Transactions on Ultrasonics, Ferroelectrics and Frequency Control*, **Volume** 49, pp. 319-326, Marchs 2002
2. D. Brei and J. Blechschmidt, Design and static modeling of a semicircular polymeric piezoelectric microactuator, *Journal of Microelectromechanical Systems*, **Volume**, 3, pp.106-155, September 1992.
3. S. Xu and T. Koko, Finite Element Analysis and design of actively controlled piezoelectric smart structures, *Finite Elements in Analysis and Design*, **Volume** 40, pp. 241-262, 2002.
4. W. Moussa, MEMS design optimization with FEA, *ALGOR Center for Mechanical Design Technology White Papers*, 2006.
5. Hong, E, R.L. Smith, S.V. Krishnaswamy, C.B. Freidhoff and S. Trolier-McKinstry, Stress Development in PZT/ZrO2/SiO2 Stacks For MEMS Piezoelectric Unimorph Diaphragms Using Interdigitated Transducer (IDT) Electrodes, 2003
6. *CRC Materials Science and Engineering Handbook*.
7. *IEEE Transactions on Electron Devices*, vol. 70, p. 421, May 1982.
8. *IEEE Transactions on Electron Devices*, vol. 25,p. 1249, October 1978.
9. *Thin Solid Films*. 1996.
10 Y. K. Hong, H.-K. Park, S. Q. Lee, K. S. Moon, R. R. Vanga, and M. Levy, Design and performance of a self-sensing, self-actuating piezoelectric monomorph with interdigitated electrodes, *Proceeding of the SPIE International Conference on Opto-mechanical Actuators, Sensors and Control*, **Volume**, 5602, pp. 210–217, October 2004.

9. Acknowledgements

The authors would like to thank Northrop Grumman Corporation for support.